Science of the Total Environment 947 (2024) 174424

Contents lists available at ScienceDirect

Science of the Total Environment

journal homepage: www.elsevier.com/locate/scitotenv

Spatiotemporal changes of urban vacant land and its distribution patterns in shrinking cities on the globe

Tangqi Tu [a], Xinyu Wang [a], Ying Long [a,b,*]

[a] School of Architecture, Tsinghua University, Beijing, China
[b] Hang Lung Center for Real Estate, Key Laboratory of Ecological Planning & Green Building, Ministry of Education, Tsinghua University, Beijing, China

HIGHLIGHTS

- Urban vacant land in 497 shrinking cities on the globe has been identified.
- The area and ratio of urban vacant land have increased worldwide from 2016 to 2021.
- Spatial distribution patterns of urban vacant land are categorized into six types.
- Variation characteristics of urban vacant land reflect socioeconomic differences.
- The ratio of urban vacant land presents a phased change in the urbanization process.

GRAPHICAL ABSTRACT

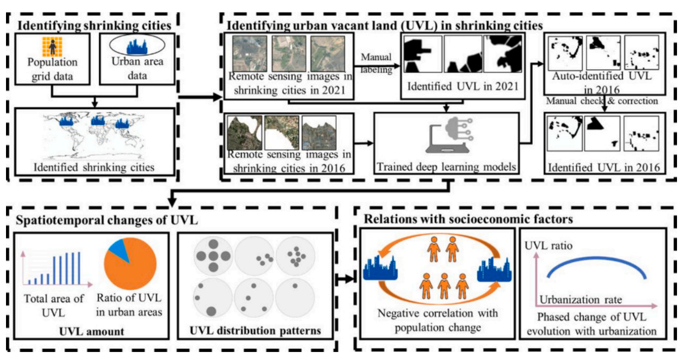

ARTICLE INFO

Editor: Shuqing Zhao

Keywords:
Urban vacant land
Shrinking cities
Spatiotemporal changes
Distribution patterns
Sustainable urbanization

ABSTRACT

Urban vacant land (UVL) has been an important issue in the urbanization process, especially for shrinking cities. Identifying UVL and analyzing its spatiotemporal characteristics are the foundation for coping with this issue. This study identified UVL in 497 shrinking cities on the globe (10 % of shrinking cities in total) in 2016 and 2021 using manual labeling and deep learning to reflect the distribution patterns of UVL and its spatiotemporal changes. The results reveal that a global expansion of UVL from 2016 to 2021 in 497 shrinking cities, with diverse distribution patterns and varying changes across different regions. As for socioeconomic factors, UVL is related to population shrinkage, and the UVL ratio presents a phased change with the increase of the urbanization rate, revealing an inverted U-shaped relationship between the UVL ratio and the urbanization rate. The distribution patterns of UVL also vary globally in different urbanization phases. This study can provide theoretical and practical insights for improving urban planning and promoting sustainable urbanization.

1. Introduction

Rapid urbanization brings great benefits but also challenges to sustainable development of cities (Cheng et al., 2022). However, under the backdrop of rapid urbanization, there are unignored shrinking cities that have become a substantial issue worldwide due to globalization and population aging (Pallagst, 2009; Martinez-Fernandez et al., 2012; Park et al., 2021; Liu et al., 2022). Under the low fertility rate and population

* Corresponding author at: Room 501, New Architecture Building, School of Architecture, Tsinghua University, Beijing 100084, China.
E-mail addresses: tutangqi@mail.tsinghua.edu.cn (T. Tu), wangxy20@mails.tsinghua.edu.cn (X. Wang), ylong@tsinghua.edu.cn (Y. Long).

https://doi.org/10.1016/j.scitotenv.2024.174424
Received 28 January 2024; Received in revised form 27 June 2024; Accepted 30 June 2024
Available online 3 July 2024

immigration, a quantity of developed and developing countries, typically with relatively higher urbanization rate, have faced severe shrinking city phenomena and population decline in the past decades and may continue in the next decades (Frazier and Bagchi-Sen, 2015; Meng et al., 2021a; Wang et al., 2022a; Zhai et al., 2022; Wang and Long, 2023; Yu and Lee, 2023). As Batty (2022) pointed out, "cities will no longer be classified by their size but by their internal dynamics". Thus, it is crucial to understand how urban space has changed in shrinking cities so that planners and decision-makers can take active actions for a sustainable future.

The decline of citizens' demand in shrinking cities may lead to low-density land development, low-efficiency land use, and the emergence of a large amount of urban vacant land (UVL) in urban space, presenting environmental and socioeconomic challenges to urban sustainability (Anderson and Minor, 2017; Smith et al., 2017). Combined with population loss, shrinking cities have confronted even more severe environmental and socioeconomic problems caused by UVL (Lokhande and Xie, 2023; Katz and Carey, 2014). Without adequate development planning, UVL may diminish urban space quality and enhance the risk of population loss, which may continuously decline the demand and bring more UVL (Li and Long, 2018; Ma et al., 2023). On the other hand, UVL can be utilized as potential resources for improving urban environment (Anderson and Minor, 2017, 2019). It is thus necessary to pay more attention to UVL in shrinking cities to promote global sustainable urbanization. Identifying UVL and analyzing its spatiotemporal characteristics in shrinking cities are the basis for planning responses. To optimize planning policies to address the issue of UVL in shrinking cities, it is necessary to identify UVL in shrinking cities and analyze its spatiotemporal changes first.

However, the UVL datasets are varied in different countries, which cannot support global-scale research to summarize universal findings for the sustainable development of shrinking cities. For instance, in China, there is no public official UVL statistical dataset (or dataset with similar content) for conducting research; in the USA, UVL datasets are stored in every local government, researchers have to connect each government to construct a database for analyzing (Song et al., 2020). Moreover, the difference of the definition and time span of UVL datasets between governments can be also a barrier for research.

To address the necessity, several methodology studies, mainly concentrated in the identification or acquisition of UVL data, have been released. These methods can be categorized into five types, including official statistics, field investigation, open-source crowdsourcing, aerial photography, and remote sensing image interpretation. These methods all have advantages and disadvantages. Official statistics have better accuracy but the availability and covering extent are very limited, and the standards are very different in various regions (Newman et al., 2016; Pearsall, 2017; Smith et al., 2017; Katz and Carey, 2014). Field investigation also has better accuracy but the covering extent is very limited, and the labor and economic costs are very high (Kim et al., 2018). Open-source crowdsourcing data have a lower cost, but have lower accuracy, and the covering extent is very limited, relying on the uploads by users (Xu and Ehlers, 2022). Aerial photography has better accuracy, but the cost is very high, and the covering extent and image size are very limited (Shukla and Jain, 2020; Sperandelli et al., 2013). Remote sensing image interpretation has better accuracy, larger covering extent, lower cost, and the only limitation is the required website and software, which can be solved more easily (Xiong et al., 2021; Li et al., 2018; Sperandelli et al., 2013; Yuan et al., 2021; Wang et al., 2022b). Also, remote sensing images are very suitable for studying cities on the globe based on a unified identification standard at a large spatial scale. Therefore, the identifying method of UVL in this study is remote sensing image interpretation.

Some methods have been used for analyzing distribution patterns of UVL in cities. Typically, Lee et al. (2018) compared the distribution patterns of UVL in Fort Worth and Chicago in the USA based on land use inventory data, and analyzed their socioeconomic and environmental factors; Li et al. (2019) used Landsat remote sensing images to interpret and analyze the spatial distribution pattern of UVL in Changchun City from 1990 to 2016, and found that there was more UVL at the edge of the city; Mao et al. (2022) used high-resolution remote sensing images to identify and analyze the spatial distribution pattern of UVL in 36 major cities in China in 2019, and found that larger cities often have higher UVL ratios; Song et al. (2020) selected 65 cities in the USA, 2 cities in Canada, and 1 city in China to analyze distribution patterns of UVL, and discovered that significant spatial differences in UVL exist at parcel, city, and country levels.

However, previous studies still need improvement. First, previous studies mainly focus on general cities or growing cities, the specific research on shrinking cities is inadequate (Song et al., 2020; Lee et al., 2018). Second, previous studies mainly analyze UVL in only a few cities in a single country, lacking large-scale and high-precision research at the global scale reflecting worldwide differences, which may be limited in the spatial dimension. In most studies, fewer than 150 cities, even only one or two cities, were analyzed, limited to one country (Lee et al., 2018; Li et al., 2019; Pearsall, 2017; Xu and Ehlers, 2022; Xiong et al., 2021; Newman et al., 2016; Mao et al., 2022; Smith et al., 2017). Besides, although some researchers have attempted to compare UVL between cities of different countries (Song et al., 2020), the time span is concentrated on a single year lacking multi-year change analysis, which may be limited in the temporal dimension. The studied countries and cities are both relatively few for global research. Furthermore, previous studies lack adequate quantitative analysis of the relationship between socioeconomic factors and UVL considering regional differences around the world (Li et al., 2019; Mao et al., 2022).

Given these research gaps mentioned above, this study aims to reveal the distribution of UVL in shrinking cities, and the relationship between temporal changes of UVL and socioeconomic factors from a global perspective. The detailed steps of our analysis are as follows. First, UVL in 497 shrinking cities of 45 countries distributed in various regions of the world is analyzed to have a comprehensive understanding of UVL distribution at the global level. Second, the temporal changes of UVL around the world are analyzed to reveal the global evolution trend. Third, key socioeconomic factors and their relations with UVL are analyzed combined with regional differences to reach a deeper understanding of the formation and dynamics of UVL on the globe.

2. Methodology and data

2.1. Definition of principal concepts

2.1.1. The definition of shrinking cities

Based on relevant research (Delken, 2008; Oswalt and Rieniets, 2006), shrinking cities are cities with a population over 10,000 that have experienced a structural crisis of population loss, economic decline and related social issues (Wiechmann, 2008; Martinez-Fernandez et al., 2012; Wang and Long, 2023). The Shrinking Cities International Research Network (SCIRN) utilizes population loss over a certain time span as an indicator to identify shrinking cities (Hollander et al., 2009; Pallagst, 2009).

Furthermore, when utilizing multiple open-source datasets to identify shrinking cities, the definition of the city boundary serves as another crucial factor not only in recognizing shrinking cities but also in separating UVL from rural vacant land and wilderness (Meng et al., 2021a; Zhai et al., 2022). The conception of natural city, which means spatially clustered geographic elements, such as POIs, road junctions or artificial impervious areas, can reflect urbanized areas better than administrative or statistical units (Long et al., 2018; Li et al., 2020). Therefore, it is more accurate to utilize natural city boundaries and high-resolution population distribution data for the identification of shrinking cities at the global scale.

2.1.2. The definition of UVL

The accurate identification of UVL relies crucially on its definition. Based on existing literature, UVL refers to land that is in a vacant state within the city (Xu and Ehlers, 2022; Smith et al., 2017): In terms of the location, UVL is mainly located within the built-up area of a city; in terms of physical spatial characteristics, UVL has no or very few buildings; in terms of functional usage, UVL does not serve stable economic and social activities or functions.

UVL presents an inactive and uncertain state, compared with an active and stable functional space in the city: From the perspective of physical form, UVL is manifested as vacant areas in urban built environment; from the temporal perspective, UVL may exist in the gaps between land use changes, which means it might have been abandoned as vacant land in the past or might be currently being developed to prepare for future use (Kim et al., 2018); from the perspective of land use, whether the land is in a stable state of utilization is a fundamental criterion for identifying UVL (Song and Li, 2019).

Based on the above definitions (Xu and Ehlers, 2022; Smith et al., 2017; Kim et al., 2018; Song et al., 2020), 3 categories and 8 subcategories of UVL have been clearly divided for the identification in remote sensing images, as shown in Table 1 and Fig. 1. For avoiding confusion, 11 non-UVL categories of urban land use that might be more likely misled to UVL are clearly delineated based on relevant references (Li et al., 2019; Smith et al., 2017), as shown in Fig. 2.

2.2. General framework

The general framework of this study is shown in Fig. 3.

First, based on the method in existing research, shrinking cities on the globe are identified based on population grid data and urban extent data of natural cities on the globe using spatial overlay analysis and calculation.

Second, according to related research, we clarify the definition of UVL and form a list for UVL classification. Based on these works, UVL in shrinking cities on the globe are identified using manual and deep learning methods. In this process, UVL patches in 2021 are firstly identified totally by manual vectorization, while UVL patches in 2016 are auto-identified by the deep learning model trained by UVL patches in 2021 with corresponding remote sensing images, followed by the manual check and correction.

Third, multiple indicators reflecting the amount characteristics of UVL are calculated, and various types of distribution patterns in all the studied cities are summarized.

Table 1
Categories and characteristics of UVL.

Categories	Subcategories	Vision characteristics
Unused land with potential development value	Bare land	Appearing brown or yellow in a soil state with little or no vegetation
	Weedy land	Light green, or with brown and yellow patches, with plenty of weed
	Other disordered vegetation	Dark green, brown or yellow, with weed and a few trees
Land within urban areas but not suitable for development	Steep exposed slopes	Attached to the mountain in the city exposed with the surface of the soil
	Waterfront areas with flood risks	Adjacent to water, exposed soil or disordered vegetation
Land that was developed or is being developed but in a vacant state at the moment	Demolished buildings	Hardened ground with traces of building demolition foundation
	Early construction sites	Appearing building foundation and construction
	Temporary stacking of materials	Temporary stacking of various materials (sand, building materials, mining slag, wood, containers, garbage, etc.) without stable land function

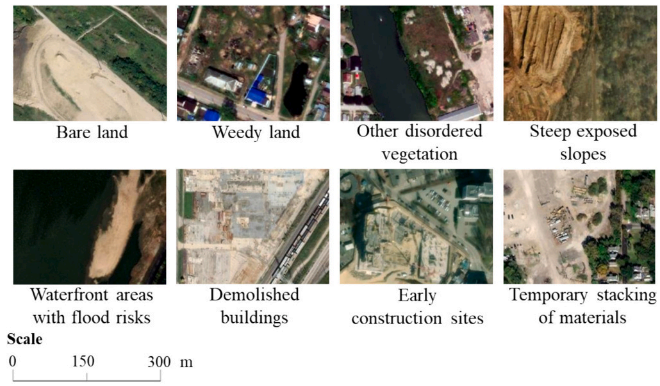

Fig. 1. UVL subcategories in remote sensing images.

Finally, using the calculated UVL indicators, spatiotemporal changes of UVL in shrinking cities on the globe can be presented, and their significant correlations and variation characteristics with socioeconomic factors are analyzed using the analysis of correlation and regression.

2.3. Identifying shrinking cities

In this research, the standard that we utilize for identification is that the reduction rate in the population change from 2000 to 2020 within the extent of the natural city should be greater than 5 % (Meng et al., 2021a; Zhai et al., 2022). The global population grid data in 2000 and 2020 from the WorldPop website (https://hub.worldpop.org) and the data of natural cities on the globe (Li et al., 2020) are used to calculate the population change and identify shrinking cities. The data of natural cities on the globe can be downloaded from the dataset of global urban boundaries (GUB) (https://data-starcloud.pcl.ac.cn/). The spatial extent of each natural city in 2000 is used to make intersections with the global population grid data to obtain the population change of each natural city between 2000 and 2020. Cities with a population loss of more than 5 % are identified as shrinking cities.

In total, 4972 shrinking cities on the globe are identified, and the total area is 38,361.86 km^2. The average area of these cities is 7.72 km^2. We randomly select 497 shrinking cities with the natural city area exceeding 5 km^2 for sampled research, which are 10 % of the total number of shrinking cities on the globe (Fig. 4). The total area of the 497 natural cities is 9737.64 km^2, and the average area is 19.59 km^2. The average change rate of the population is −13.97 %. The maximum of the natural city area is 972.30 km^2 (Cleveland, Ohio, USA), and the minimum is 5.01 km^2 (Qingyuan, Zhejiang, China). Although each country may have a different number of cities, the number of sampled cities largely relies on the total number of cities in each country, which are generally proportional. Therefore, these sampled shrinking cities can reflect the general characteristics and relative amount of the urban vacant land in all the shrinking cities across countries.

2.4. Identifying urban vacant land (UVL)

2.4.1. General process

As shown in Fig. 5, the identification process can be summarized as three main steps, including manual labeling, auto-identifying and manual correction. The source of remote sensing images is the World Imagery website (https://desktop.arcgis.com/en/imagery/). The remote sensing images within the extent of the 497 natural cities in 2016 and 2021 are downloaded by the Bigemap software (https://www.bigemap.com/) with a precision of 1.19 m.

2.4.2. Manual labeling

For the step of manual labeling, the ArcGIS software is used to

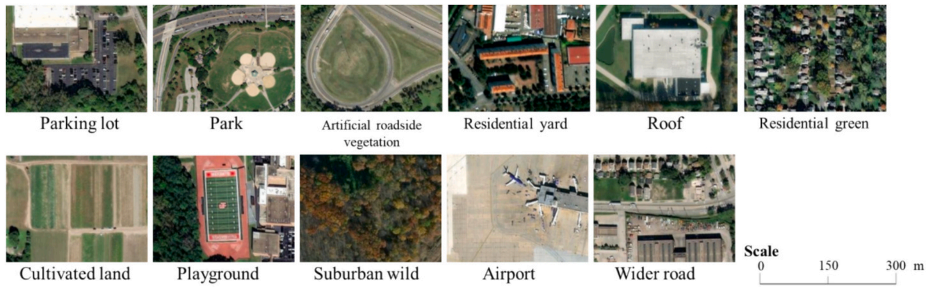

Fig. 2. Non-UVL categories in remote sensing images.

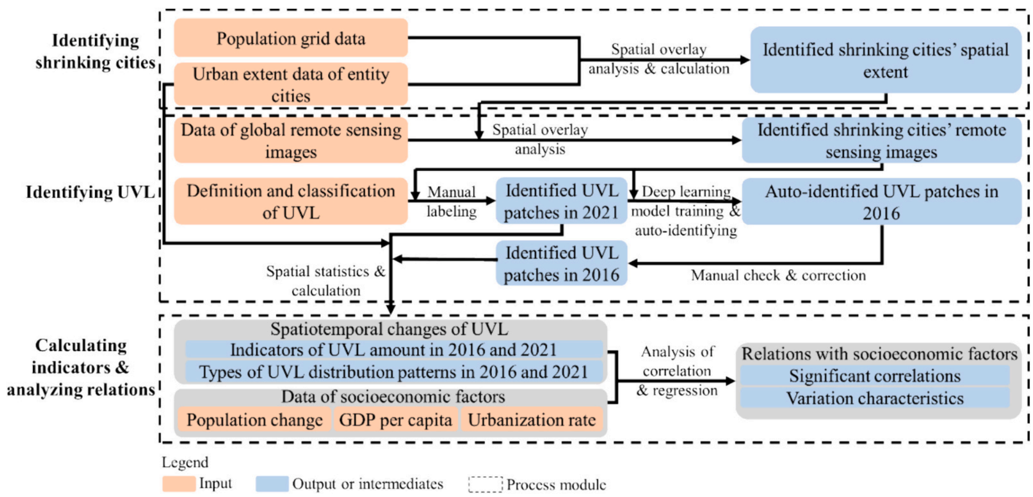

Fig. 3. General framework of this study.
Note: UVL = urban vacant land.

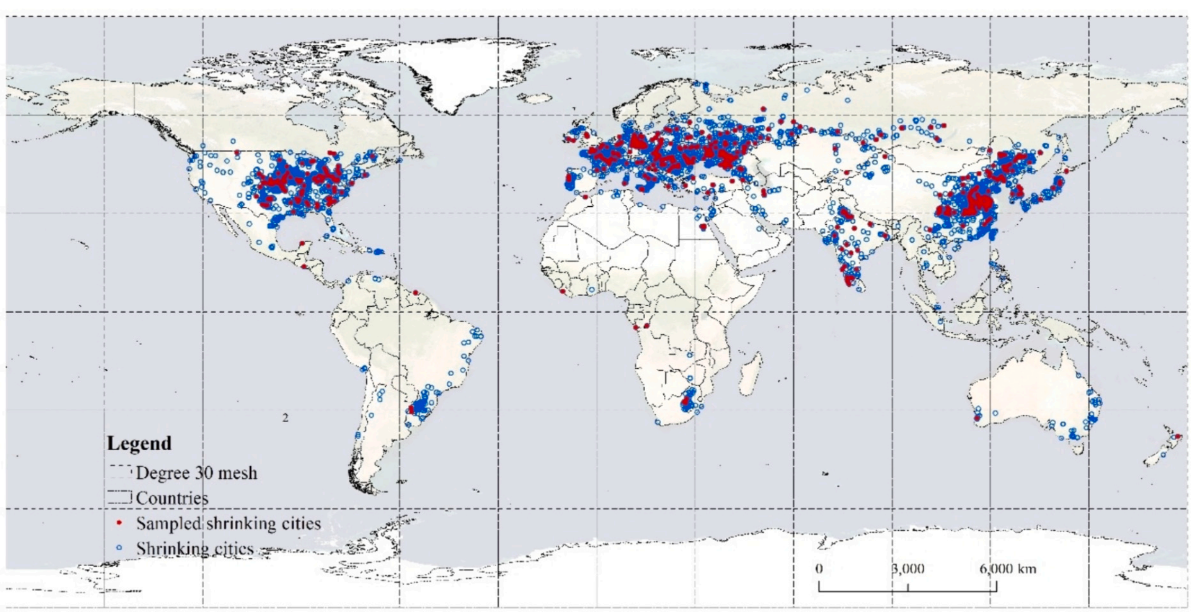

Fig. 4. Identified and sampled shrinking cities on the globe of this study.

manually label UVL by vectorizing raster patches that fit the definition of UVL in remote sensing images of all 497 cities in 2021. First, the remote sensing images within the natural city areas of selected shrinking cities in 2021 are downloaded. Second, all the images are divided into raster patches with a resolution of 2520 * 2520 for subsequent processing. This resolution is suitable as input for the DeeplabV3 model (Mao et al., 2022). This step was carried out using ArcGIS software. We selected 2620 raster patches of remote sensing images to conduct manual labeling for training our deep learning model. Then, the first author conducts the manual labeling by vectorizing defined UVL patches

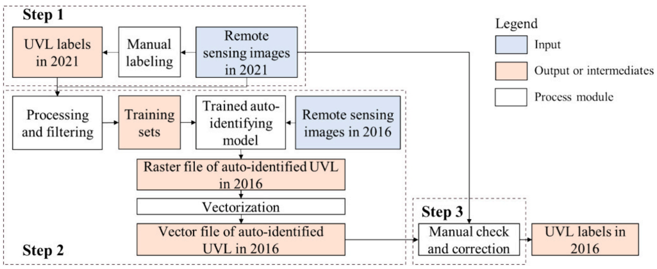

Fig. 5. General procedures of identifying UVL.

in the remote sensing image of each city one by one with the tool "Create Features" in the ArcGIS software. When all the UVL patches of a city are vectorized, the same action is repeated for the next city. The working period of the manual labeling is from the middle of October 2022 to the middle of February 2023, lasting for more than four months. All the vectorized labels of UVL in 2021 are examined by the second author for the preparation of training the auto-identifying model.

2.4.3. Auto-identifying

For the step of auto-identifying, a deep learning model is trained to automatically identify UVL in 2016 using the manual labels in 2021. The basic training framework used in this study is the DeepLabV3 model, which has proved to be suitable for image semantic segmentation and been widely adopted (Chen et al., 2019). The codes for training and auto-identifying in this model is based on the existing research by Mao et al. (2022).

First, based on the manual labeling result (2620 raster patches of remote sensing images with their manual labels), the vectorized UVL labels in the manual labeling are rasterized into images. These images, with a resolution of 2520 * 2520, are used for model training. Furthermore, we removed images without UVL, resulting in a final dataset of 1877 images.

Second, cities are categorized for training best models. Considering the geographical environment varies significantly among cities on the globe, training a single deep learning model might be incompatible for all the cities. Thus, it is necessary to categorize cities and train the corresponding deep learning model for each city category. According to previous studies (Song et al., 2020; Mao et al., 2022) and our careful observation of the UVL patches in the remote sensing images of all the 497 cities, it can be seen that the physical appearance of UVL is largely related to the characteristics and distribution of vegetation and soil mainly influenced by climate. Combining the Köppen-Geiger climate classification maps at 1-km resolution (Beck et al., 2018) with the location of each city, the 497 cities are categorized into five categories: desert (10 cities), savanna (52 cities), forest (326 cities), summer-dry (16 cities), and winter-dry (93 cities).

Third, images for training sets are selected. Given that an excessive number of images with extremely sparse UVL labels can be detrimental to the model's training efficacy (Mao et al., 2022), the images in each category are filtered based on the UVL ratio (relative to the image area). Ultimately, the top 5 % of images showcasing the highest UVL ratios are chosen for training in each category, amounting to 200 images in total (comprising 100 remote sensing images and their corresponding UVL label images in 2021). To verify the effectiveness of training multiple models by categories, a single model based on all the selected images without categorization is also trained.

Then, the deep learning models are trained and utilized using the selected images as the training sets for auto-identifying UVL in 2016. The generated training set of each category is trained with the DeepLabV3 model in the programming platform of PyCharm. This model functions in three programs. The first program runs for obtaining the UVL rate of the input training set, which is the proportion of the pixels of UVL to the total pixels in the UVL label images. The second program automatically trains an auto-identifying model using the input training set and UVL rate from the first program. The third program automatically utilizes the model trained by the second program to identity UVL patches in the remote sensing images. To evaluate the trained model performance, the F_2-score and *IOU* (intersection over union) value are introduced. The formulas are (Duque et al., 2017; Mao et al., 2022):

$$F_2 = 5 \cdot \frac{precision \cdot recall}{(4 \cdot precision) + recall} \tag{1}$$

$$precision = \frac{TruePositives}{TruePositives + FalsePositives} \tag{2}$$

$$recall = \frac{TruePositives}{TruePositives + FalseNegatives} \tag{3}$$

$IOU = \frac{area(A \cap B)}{area(A \cup B)}$ (4)where F_2 is the F_2-score that represents the general performance level of a trained model; *precision* represents the proportion of the true UVL to all the UVL identified by a trained model, indicating the accuracy; *recall* represents the proportion of the true identified UVL to all the true UVL, indicating the capability of covering the true UVL; *IOU* represents the proportion of the area of the intersection between the true UVL and identified UVL to the area of the union of these two. Higher values of F_2-score and *IOU* indicate better performance of the trained model.

The information of the trained models for the five city categories is shown in Table 2. The average values of F_2-score and *IOU* of the five categorized models are 0.860 and 0.635, respectively. The non-categorized model has lower values in these two parameters. This shows that training by categories can achieve better performance than without categorization. It can be seen that trained models can reflect the general spatial distribution of UVL from the samples (Fig. 6).

The innovativeness of this identification method is primarily demonstrated through the development of deep learning models based on training sets from cities worldwide. Most of the existing studies identifying UVL are solely conducted by human visional identification based on case studies, limited in efficiency and accuracy, while the adoption of deep learning models is very rare (Lee et al., 2018; Li et al., 2019; Pearsall, 2017; Xu and Ehlers, 2022; Xiong et al., 2021; Newman et al., 2016; Song et al., 2020; Smith et al., 2017). Only a few researchers adopted deep learning models limited to one country, which may be not suitable for various cities across different countries. Additionally, the number of cities analyzed using deep learning models in existing research is significantly smaller than in this study (Mao et al., 2022). As shown in Appendix C, the performance metrics of deep learning models in this study are close to those in the existing research, demonstrating advantages in identifying UVL across a more diverse range of countries and cities.

The auto-identified UVL labels produced by the trained models are in the format of raster images, which are subsequently processed for georeferencing and vectorization by running the ArcPy programs for about 99 h in total. However, although auto-identifying can generally locate UVL patches, it is very necessary to conduct manual check and correction for the maximized accuracy in the patch shapes and distribution of UVL.

2.4.4. Manual check and correction

For the step of manual check and correction, the identified UVL results undergo several rounds of manual check and correction by multiple researchers to ensure accuracy and consistency. In the first round, the authors individually conduct a thorough check of all results and make necessary corrections. In the second round, the identified results for all the natural cities are independently reviewed by four additional researchers to mitigate subjectivity. The authors correct the results according to their feedback. In the third round, the identified results of 497 cities are randomly distributed to ten researchers for checking, and each researcher is assigned to check about 50 cities on average. These

Table 2
Information of trained deep learning models for auto-identifying UVL.

Trained model	F_2-score	IOU	Loss	Epoch	UVL rate of training set	Code running duration
Desert	0.892	0.757	0.230	25	0.117	1.5 h
Savanna	0.846	0.591	0.192	32	0.140	2 h
Forest	0.846	0.608	0.228	40	0.160	19 h
Summer-dry	0.877	0.654	0.279	27	0.250	2 h
Winter-dry	0.837	0.563	0.204	33	0.139	6 h
Non-categorized	0.820	0.546	0.261	31	0.160	30 h

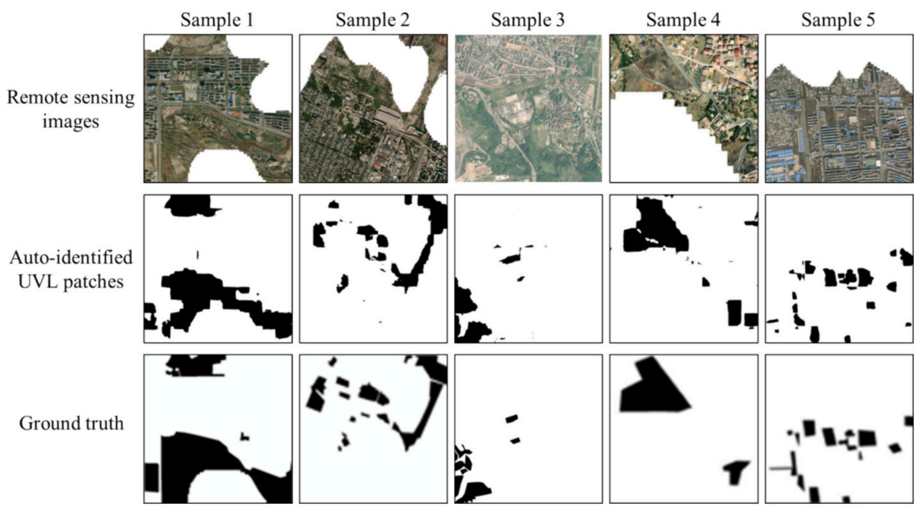

Fig. 6. Samples of auto-identified UVL patches.

researchers are all working in the field of urban space studies. Based on their feedback, the authors correct the results for another time. Finally, the authors observe all the UVL patches in each city one by one carefully to see if these researchers have omitted some places. It can be found that major bias is from extremely small polygons mostly smaller than 1 m^2, which are mainly produced by occasional deviation of human vision. By comparing the results after the final thorough check as the ground truth with the results from the feedback of other researchers, it can be calculated that the F_2-score and *IOU* of manual working based on others' feedback are both over 0.999, which have reached very high values.

2.5. Identifying UVL distribution pattern types

The spatial distribution patterns of UVL can reflect the characteristics of UVL in different regions. According to the classification criteria of shrinking city research, existing studies have categorized the population loss patterns of shrinking cities into six types: periphery, partial, scatter, overall, sparse, and central, based on observing the identification results in combination with existing literature (Blanco et al., 2009; Schetke and Haase, 2008; Meng et al., 2021b). We have adopted these classification criteria and applied them to analyze the distribution patterns of vacant land in shrinking cities. The general illustration for each type is shown in Fig. 7, and typical cities of these UVL distribution pattern types are shown in Fig. 8.

The specific characteristics of these types are as follows. In the overall type, UVL is widely distributed in various parts of the city. In the partial type, UVL is concentrated in a specific part of the city (excluding the central part) or particular areas. In the central type, UVL is concentrated in the city's central zone. In the periphery type, UVL is extensively distributed around the periphery of the city. In the scatter type, UVL is scattered throughout the city in few and small patches. In the sparse type, the number and area of UVL in a city are very small. The classification of these types is conducted by manually observing the spatial distribution characteristics of UVL in all the cities one by one

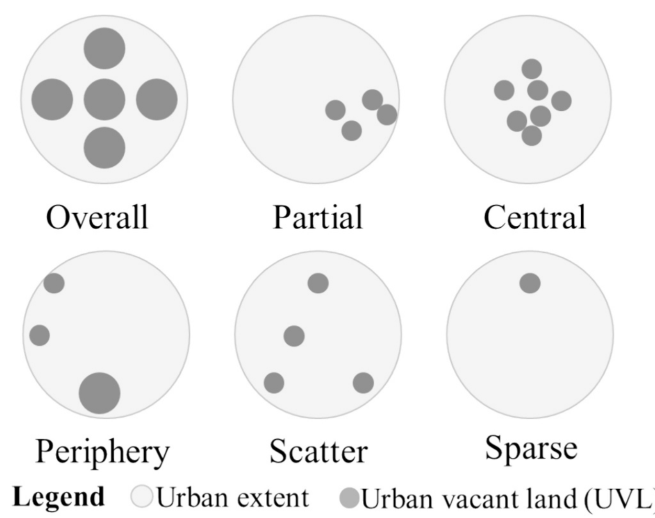

Fig. 7. General illustration of UVL distribution pattern types.

according to the method of existing literature (Meng et al., 2021b). Three key factors are considered in the classification, including the amount, proportion, and agglomeration. The classification is finished through several rounds. In the first round, if the amount of UVL is small for a city, the spatial distribution pattern can be classified into the sparse, partial or scatter type based on the agglomeration degree and number of patches. Otherwise, it turns to the second round. In this round, if the proportion of the UVL in the inner or outer part of a city is significantly higher, the spatial distribution pattern can be classified into the central type or periphery type. If the difference of the proportions is not obvious, the overall or partial type can be ultimately determined based on the agglomeration degree.

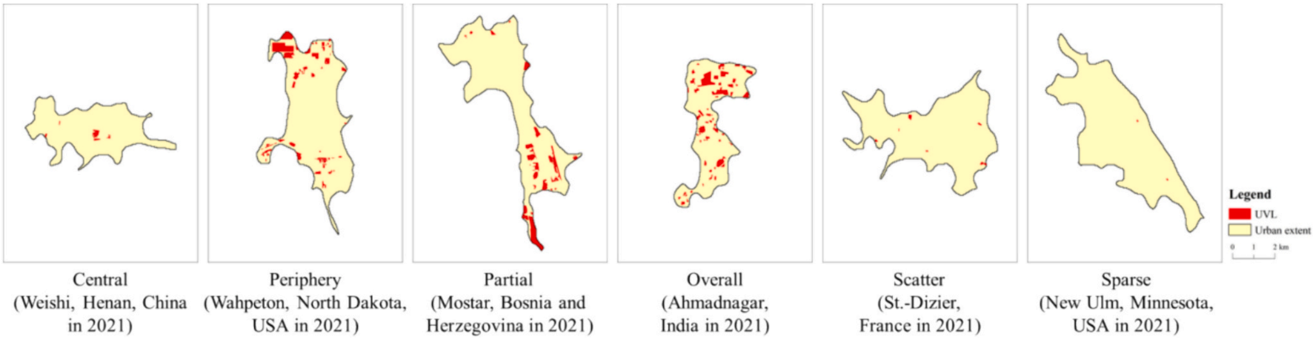

Fig. 8. Typical cities of various UVL distribution pattern types.

2.6. Calculating indicators and analyzing relations

Two indicators reflecting the amount characteristics of UVL are the total area of UVL (total area) and the proportion of UVL to the urban area (UVL ratio). The UVL ratio can reflect the severity of the UVL issue for the entire city considering the urban area. The total area of UVL can be calculated based on the accumulation of all the UVL patches within the urban spatial extent, while the UVL ratio needs more calculation steps. The formulas utilized for calculating UVL ratio are:

$$R_i = \frac{TA_i}{UA_i} \tag{5}$$

$$R_j = \frac{\sum TA_{i,j}}{\sum UA_{i,j}} \tag{6}$$

where R_i is the UVL ratio of the sampled shrinking city i; TA_i is the total area of UVL in the sampled shrinking city i; UA_i is the urban area of the sampled shrinking city i; R_j is the UVL ratio of all the sampled shrinking cities in region j or country j; $TA_{i,j}$ is the total area of UVL in the sampled shrinking city i in region j or country j; $UA_{i,j}$ is the urban area of the sampled shrinking city i in region j or country j.

Utilizing calculated UVL indicators, we conduct a comprehensive analysis of their relationship with socioeconomic factors, such as population, GDP and urbanization rate (Table 3). Previous studies have shown that economic status, urbanization, and population migration may affect the amount or distribution of UVL (Lee et al., 2018; Song et al., 2020). Economic status might affect the capacity to develop vacant land in cities. Urbanization may lead to urban land use changes. Population migration could impact the demand for urban land resources. The urbanization rate is defined as the proportion of the urban population to the total population (Fan et al., 2019). First, at the city level, we examine correlations between UVL indicators and population changes using Spearman correlation coefficients. Then, at the country level, we explore correlations between UVL indicators and socioeconomic factors such as GDP per capita and urbanization rate, employing the Spearman correlation coefficients. Finally, we conduct regression analysis to further investigate indicators that exhibit stronger correlations at the country level, aiming to have a deeper understanding of UVL changes. The regression analysis is weighted by the number of cities in each country to reflect the general characteristics of all the studied cities. Weighted regression, or weighted least squares, is a regression model where each observed value is given a certain weight that tells the statistical software how important it is in the model fit (Gelman et al., 2020). In this study, the regression calculation is processed by the IBM SPSS software. The socioeconomic dataset at the country level is from the World Bank database, and the website is https://databank.worldbank.org/home.aspx.

Table 3
Indicators for correlation analysis.

Level	Type	Indicator
City	Socioeconomic factors	Population change number
		Population change rate
	UVL	Total area of UVL in 2016
		UVL ratio in 2016
		Total area of UVL in 2021
		UVL ratio in 2021
Country	Socioeconomic factors	GDP per capita in 2016 and 2021
		Urbanization rate in 2016 and 2021
	UVL	UVL ratio (standardized natural logarithm) in 2016 and 2021

3. Results

3.1. Analysis of spatiotemporal changes in UVL

3.1.1. Spatiotemporal changes in UVL amount

In total, this study has confirmed 13,544 UVL patches, with 8879 UVL patches in 2021 and 4665 UVL patches in 2016. In all the identified vacant land, the largest, the smallest, and the average area are 3.88 km^2, 204.84 m^2, and 3.98×10^4 m^2, respectively. The top 95.26 % of all the identified vacant land patches are over 1800 m^2, and only fewer than 5 % are smaller than 1800 m^2. Table 4 shows indicators of UVL amount in sampled shrinking cities in 2016 and 2021 at the regional and global level. Since the sampled shrinking cities in Oceania are only two, they are merged into the region "Asia and Oceania" based on the regional division of the United Nations (UNIDO (United Nations Industrial Development Organization), 2022). From 2016 to 2021, the total area of UVL has increased by 52.25 %, which shows the obvious expansion of UVL in sampled shrinking cities on the globe (Table 4). At the regional level, discernible disparities are evident. From the perspective of the total area and ratio of UVL, there has been an overall increase, primarily driven by Europe and Asia for the vast majority of the urban area. The total area of UVL has substantially increased in sampled shrinking cities in Asia.

At the country level, the countries with prominent issues of vacant land in their cities are generally major countries in Eastern Europe, East Asia, South Asia, and the USA. The more detailed information about these UVL indicators at the country level is shown in Appendix A. It is

Table 4
Indicators of UVL amount in sampled shrinking cities in 2016 and 2021 at the regional and global level.

Region	Number of sampled shrinking cities	Total area (km^2)		UVL ratio (%)	
		2016	2021	2016	2021
Africa	13	2.10	6.05	0.61	1.76
The Americas	98	33.07	48.69	1.47	2.16
Asia and Oceania	162	60.87	119.42	2.20	4.32
Europe	224	117.87	151.52	2.69	3.46
Global	497	213.91	325.68	2.20	3.34

noted that both China and India have UVL expanding rapidly in the total area.

At the city level, the levels of UVL indicators are uneven across cities around the world, as shown in Fig. B1 to Fig. B4 in Appendix B. For the distribution of the total area of UVL, cities with a larger UVL area are mainly distributed in central and southwestern Russia, as well as some regions of China. Cities with a high UVL ratio are mainly located in eastern and central Europe, northern USA, China and India. Among them, from 2016 to 2021, the UVL ratio in Chinese and Indian cities has significantly increased. By calculating the change rate of the total area of UVL from 2016 to 2021, it can be seen that the cities with crucial growth in UVL are mainly concentrated in Northeast China, the Yangtze River Basin, Central India, Eastern Europe, and Central Europe (Fig. 9).

3.1.2. Spatiotemporal changes in UVL distribution pattern types

The statistical results of UVL distribution pattern types for 497 studied cities are shown in Fig. 10 and Fig. 11. Most types are partial and scatter types. At the regional level, the periphery type and overall type have increased significantly from 2016 to 2021 in Asia, indicating a substantial amount of UVL emerging at the cities' periphery. On the other hand, the increase in the central type indicates an increase in the proportion of UVL in the inner part of the city, showing a trend of inward aggregation distribution. Cities of the central type are located in Asia and Europe, while in the Americas and Oceania more cities belong to the overall type. Different characteristics of UVL distribution suggest different socioeconomic conditions between countries.

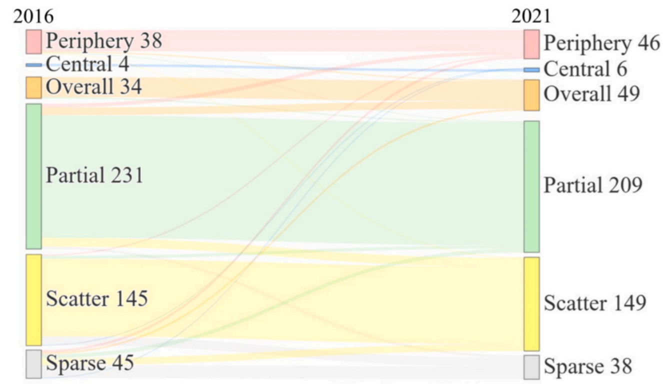

Fig. 10. Evolution flows of UVL distribution pattern types from 2016 to 2021 at the global level.

3.2. Socioeconomic factors related to spatiotemporal changes in UVL

Based on the spatiotemporal changes in UVL, this study firstly performs correlation analysis on related factors of 497 cities, including indicators of population (population change number, population change rate), economy (GDP per capita), urbanization (urbanization rate), and UVL (total area and UVL ratio). The results are shown in Table 5.

At the city level, the results showed a significant negative correlation between the population change number and multiple UVL indicators. The correlations between the population change number and total area of UVL in 2016 and 2021 are significant. This indicates the obvious connection between urban population shrinkage and UVL amount. That is, the more severe is the population shrinkage for a city, the larger is the total area of UVL.

At the country level, this study explores relations between socioeconomic indicators such as the GDP per capita as well as urbanization rate and various indicators of UVL indicators. The correlations and coefficients are analyzed and calculated. The results show that the UVL ratio has significant negative correlations with both the urbanization rate and GDP per capita. According to the Spearman coefficients, the correlation between the urbanization rate and UVL ratio is stronger.

According to the results of the correlation analysis, the urbanization rate and total ratio of UVL in 2016 and 2021 are analyzed with weighted regression based on the number of cities to further reveal the quantitative relation between these two indicators. As shown in Fig. 12, the result reveals that with the increase of urbanization rate, the total ratio of UVL generally presents the trend of first increasing and then decreasing. This trend can be illustrated as an inverted U-shaped curve. From the perspective of temporal evolution, a faster growth in the UVL ratio tends to appear in the middle or early urbanization stage, while the UVL ratio tends to increase slower or even decrease at the later

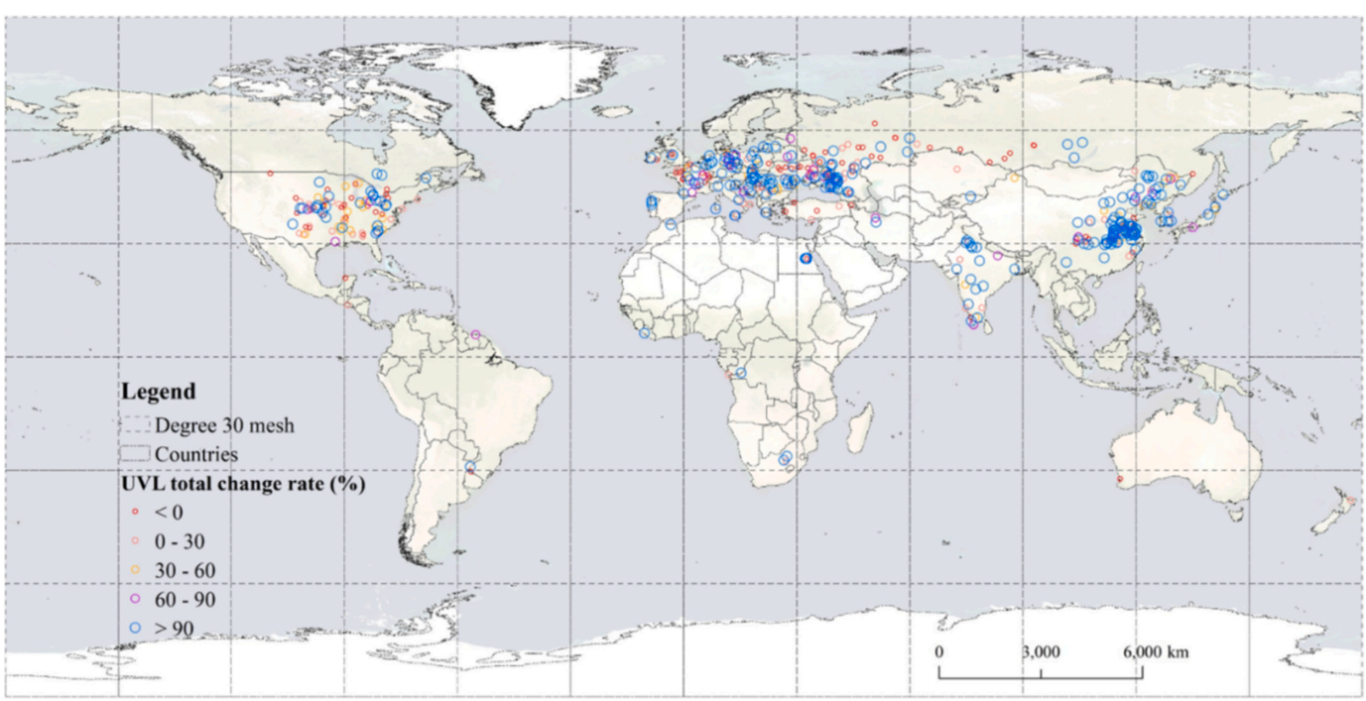

Fig. 9. Total area change rate of UVL at the city level from 2016 to 2021.

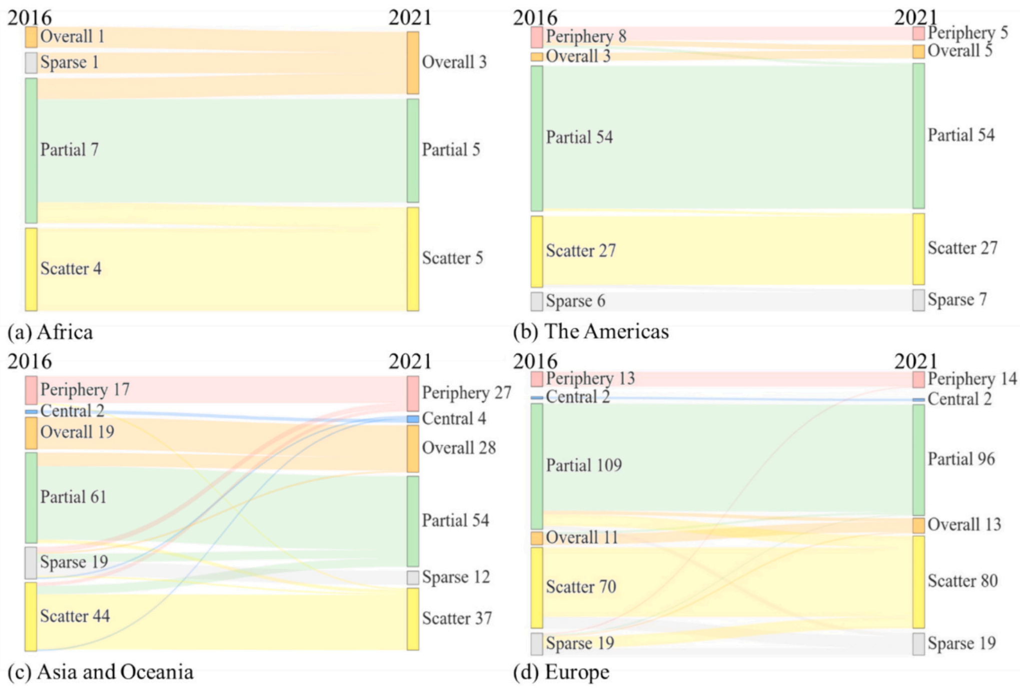

Fig. 11. Evolution flows of UVL distribution pattern types from 2016 to 2021 at the regional level.

Table 5
Spearman correlations between UVL and socioeconomic factors.

Level	Indicator	Spearman correlation	Total area of UVL in 2016	UVL ratio in 2016	Total area of UVL in 2021	UVL ratio in 2021
City	Population change number	Coefficients	−0.192*	0.114	−0.342*	0.031
		Sig. (bilateral)	0.000	0.011	0.000	0.486
	Population change rate	Coefficients	0.115	0.068	0.026	−0.050
		Sig. (bilateral)	0.011	0.129	0.557	0.266
Country			UVL ratio (standardized natural logarithm) in 2016 and 2021			
	Urbanization rate in 2016 and 2021	Coefficients	−0.264*			
		Sig. (bilateral)	0.000			
	GDP per capita in 2016 and 2021	Coefficients	−0.203*			
		Sig. (bilateral)	0.000			

* At a confidence level (bilateral) of 0.01, the correlation is significant.

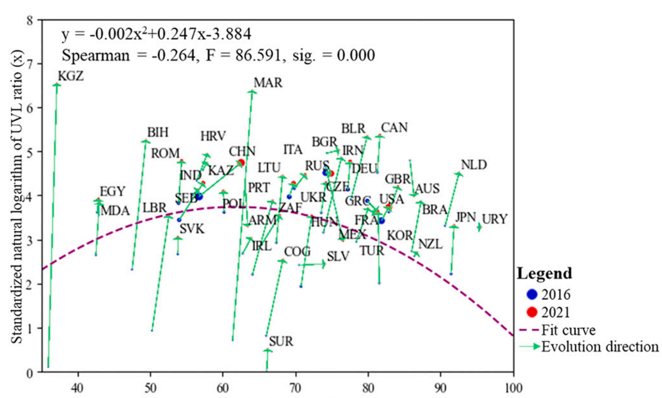

Fig. 12. Weighted regression analysis of urbanization rate and total UVL ratio. Note: Each dot represents a country, and a larger dot indicates more studied cities in that country. Three letters are the abbreviation for a country, and full names of these countries are shown in Appendix A.

urbanization stage.

4. Discussion

4.1. Spatial and temporal patterns of UVL

Previous studies have shown that both urban land expansion and urban population shrinkage can lead to the formation of UVL. On the one hand, the speed of urban land expansion is significantly faster than the speed of population urbanization in many cities, resulting in vacant land in urban areas, such as undeveloped land that has not been developed in a timely manner within the urban extent (Pagano and Bowman, 2000; Németh and Langhorst, 2014; Song et al., 2020). This indicates a severe waste of land resources in the urbanization process (Zhao et al., 2018). On the other hand, in shrinking cities, urban population shrinkage leads to insufficient utilization and management of urban land, resulting in abandoned land and demolished buildings, which can increase the area of vacant land in urban areas. This phenomenon can be more commonly seen in post-industrial cities, like many cities in the northern USA, Eastern Europe and northeast China (Martinez-Fernandez et al., 2012). Also, researchers have noted that different patterns of urban land use may reflect varied socioeconomic circumstances (Salvati et al., 2018). These studies have provided theoretical foundations, but the correlations between socioeconomic factors such as urbanization level as well as population and UVL still lack clear quantification, and specific measurement is needed to reveal the differences between cities on the globe. Thus, this study analyzes spatiotemporal changes of UVL in shrinking cities worldwide to explore variations among cities across different countries and associated socioeconomic factors. The observed trend of UVL expansion in shrinking cities globally indicates the importance of heightened attention in global urban planning practice, especially in shrinking cities.

According to the results, the distribution of UVL shows an obvious phased change across countries. The evolution process of UVL can be divided into the following stages with different spatial patterns.

In the early urbanization stage, like in some African cities, developing capacity is limited, and the speed of urban land expansion is relatively lower, resulting in the relatively lower UVL ratio and domination of the partial or scatter type. Some shrinking cities may change into the overall type with the urbanization process.

In the rapid urbanization stage, the speed of urban land expansion is much faster. However, limited to the population size and construction cost, a large area of urban land is left vacant, markedly increasing the UVL ratio in peripheral urban areas. This phenomenon can be obviously seen in the evolution trend in Asia, where the periphery type has increased by 58.82 % from 2016 to 2021. Shrinking cities in countries at this urbanization stage tend to have the largest area of UVL.

In the later stage of urbanization, like in some high-income European countries, the difference between the inner part and periphery of a city tends to become smaller, which can be seen from the increase of the scatter type, where the redevelopment may take place in urban areas, the UVL ratio tends to be lower.

However, for cities in other developed countries or regions like Canada or the northern USA, with the suburbanization process and population shrinkage, more people leave the inner areas of these cities, leading to spatial decay in the inner urban areas, resulting in the increased UVL ratio and decreased number of cities of the periphery type. For example, Cleveland is a shrinking city in the Rust Belt of the USA, and the recession of the manufacturing industries of this city has brought out the reduction of development capacity and more urban land left vacant in the central urban area (Zhai et al., 2022).

Although the UVL ratio has a general change trend with the change in the urbanization rate, the specific conditions of cities need to be considered. In some cities with high density, limited land resources and advanced economic development at the later urbanization stage, the UVL ratio may be lower because of the sufficient utilization of land use in their urban areas. For example, in many Japanese cities like Toyama, UVL can be utilized as public facilities, such as community centers and parks (Kobayashi and Ikaruga, 2016). At the rapid urbanization stage, this issue tends to be more complicated. Although more UVL will appear in cities in developing countries in general at this stage, the UVL ratio may vary between different countries resulting from the difference in land-use planning and management. For example, compared with Chinese cities, Indian cities have a lower UVL ratio on average. This could be affected by the higher proportion of slums that have occupied UVL in India and more vacant land left for real estate development in China (Sarkar and Jana, 2023; Zhang et al., 2023). Therefore, the general trend at the country level needs to be considered in combination with the specific conditions at the city level.

4.2. Management and utilization of UVL

In response to the widespread existence of UVL, the database of UVL should be established based on remote sensing images using the methods of manual auditing and deep learning to promote the efficient and reasonable use of urban land. In view of the significant correlation between population shrinkage and UVL, the monitoring of UVL in shrinking cities should be conducted or strengthened.

It is necessary to make proper use of UVL to achieve the green development transformation of shrinking cities. Here are several recommendations for decision-makers.

Recognizing the complexity of UVL in shrinking cities. UVL issues in shrinking cities are multifaceted and influenced by diverse environmental and socioeconomic factors. Decision-makers need acknowledge the complexity of UVL dynamics and create strategies that fit each city's unique situation. Temporary utilization strategies for vacant land have been implemented in Berlin, Germany and some American cities like St. Louis, Philadelphia, Detroit and Chicago to cope with the evolving urban development status in a more flexible way (Németh and Langhorst, 2014). In addition, shrinking cities like Cleveland in the USA have set up the land bank as an effective way to sell tax-reverted land for the reuse of UVL (Kim et al., 2020).

Case Studies. While this study provides valuable insights into the general distribution characteristics of UVL in shrinking cities globally, the real situations of individual shrinking cities are largely varied. Decision-makers should support further research, including in-depth case studies in representative cities, which can offer detailed insights into the underlying factors driving UVL dynamics and inform targeted policy interventions. For instance, a study on redeveloping urban vacant land through urban greening has been supported by the Basque Government in Spain (Míguez et al., 2020). Additionally, the analysis of urban space quality using mobile sensing technology has been conducted in several cities in China to support research on urban vacancy and related issues (Wang et al., 2024).

Integration of UVL Management into Urban Planning Strategies. Decision-makers should prioritize the integration of UVL management considerations into urban planning strategies. This entails developing policies that incentivize the efficient utilization of UVL, promote sustainable development practices, and mitigate the negative impacts of vacant land on urban ecosystems. For example, Scotland has proposed planning policies for vacant land as "distinctive places" within its general planning framework. These policies emphasize that local development plans should prioritize the reuse of vacant land. Furthermore, planning applications for proposals that result in the permanent or temporary reuse of vacant land should be supported in principle (Humphris et al., 2024).

Collaborative Approaches and Stakeholder Engagement. Addressing UVL issues requires a collaborative approach involving various stakeholders, including government agencies, urban planners, community groups, and environmental organizations. Decision-makers should facilitate dialogues and partnerships to develop holistic solutions that address the complex challenges associated with UVL in shrinking cities. For instance, civil society organizations (CSOs) in Boston have led a project of transforming UVL into a neighborhood pocket park, showing that public-civic partnerships have the potential to improve UVL management (Foo et al., 2013).

4.3. Limitation of this study

Despite the advantages of remote sensing imagery in identifying UVL, this study still has some shortcomings that may need to be addressed in future research.

First is the resolution limitation. The resolution of remote sensing images may not capture fine details of vacant land features, especially in high-density urban areas or complex urban environments. This may lead to the omission of small vacant land areas, thus affecting the accuracy of vacant land distribution analysis.

Second is about the occlusion issue. Objects such as buildings and trees may obstruct parts of the ground, resulting in certain areas of the remote sensing image being unobservable. This can cause misinterpretation, where obstructed ground is mistakenly identified as vacant land, or actual vacant land is partially obscured and goes unrecognized. What's more, seasonal and climatic effects also have a significant impact. Seasonal changes and varying climatic conditions can impact the quality and availability of remote sensing images. For instance, snow cover or vegetation growth may obscure the ground, making vacant land difficult to identify. Additionally, cloud cover and lighting conditions may also affect the quality of remote sensing images.

Third is the classification accuracy. Classification algorithms used on remote sensing images may introduce errors, leading to inaccurate identification of vacant land. These algorithms typically rely on pixel values, texture, shape, and other features for classification. However, in complex urban environments, there may be other features such as buildings, roads, and water bodies that resemble vacant land, increasing the likelihood of misclassification.

Fourth, the data update cycle is another shortcoming. Remote sensing images may have long update cycles, resulting in delayed identification of vacant land. In rapidly developing or changing urban areas, outdated remote sensing images may fail to accurately reflect the current distribution of vacant land, necessitating frequent data updates to maintain accuracy.

5. Conclusion

Urban vacant land (UVL) has become a prominent issue in the process of urbanization, and many shrinking cities around the world are facing severe UVL challenges. Identifying and analyzing the spatiotemporal changes of UVL in shrinking cities are the foundation for the planning response. The spatiotemporal changes of UVL include two key dimensions: the amount and spatial distribution. Based on identifying UVL in 497 shrinking cities around the world in 2016 and 2021, the findings can be summarized as follows.

First, the total area of the UVL has obviously increased in shrinking cities on the globe, and the spatial distribution of UVL is extremely uneven. Asian cities are facing the problem of rapid expansion of vacant land in urban areas. Second, a correlation exists between urban population shrinkage and the distribution of UVL. There is a significant negative correlation between the change in urban population and the UVL amount. Third, the UVL ratio is significantly correlated to the urbanization rate. With the increase of urbanization rate, the UVL ratio tends to increase first and decrease later, which presents a phased change. Fourth, similar to the UVL ratio, the spatial structure of UVL also presents different types in various countries and urbanization stages. Generally, in some developing countries experiencing rapid urbanization, more cities tend to be the periphery type in the UVL spatial distribution pattern, while in some developed countries the spatial difference of UVL within the city tends to be smaller, resulting in more cities of the scatter type. Given the complexity of shrinking cities on the globe, the general trend at the country level needs to be considered in combination with the specific conditions at the city level.

This study filled the research gap of the vacant land in shrinking cities on the globe, and formed a new perspective for enriching the theories of spatiotemporal changes of shrinking cities. The framework and findings in this study can provide a scientific reference and technological support for optimizing urban space planning policies and achieving sustainable urbanization.

CRediT authorship contribution statement

Tangqi Tu: Writing – review & editing, Writing – original draft, Visualization, Software, Methodology, Formal analysis, Data curation, Conceptualization. **Xinyu Wang:** Writing – review & editing, Visualization, Software, Methodology, Data curation, Conceptualization. **Ying Long:** Supervision, Resources, Project administration, Funding acquisition, Conceptualization.

Declaration of competing interest

The authors declare no potential conflicts of interest with respect to the research, authorship, and/or publication of this article.

Data availability

Data will be made available on request.

Acknowledgements

This research was supported by the National Natural Science Foundation of China [52178044]. We would like to thank Yan Li, Wenzhu Li, Qiao Chu, Huimin Zhao, Qi Hao, Yue Ma, Nanxi Su, Yecheng Zhang, Jianing Liang, Qizheng Wu, Junhao Xia, and Qiyuan Hong for their manual check work on the spatial data of identified urban vacant land.

Appendix A

Table A1
Indicators of UVL amount at the country level in 2016 and 2021.

Country name	Abbreviation	Number of cities	Total UVL area in 2016	Total UVL ratio in 2016	Total UVL area in 2021	Total UVL ratio in 2021	Urbanization rate in 2016	Urbanization rate in 2021
Armenia	ARM	1	0.37	3.46	0.13	1.22	63.08	63.43
Australia	AUS	1	0.30	5.45	0.13	2.41	85.80	86.36
Bulgaria	BGR	1	0.59	6.41	0.63	6.88	74.33	76.03
Bosnia And Herzegovina	BIH	2	0.08	0.46	1.57	8.63	47.52	49.43
Belarus	BLR	2	0.56	2.25	2.34	9.42	77.66	79.91
Brazil	BRA	1	0.04	0.69	0.12	2.16	86.04	87.32
Canada	CAN	6	3.92	4.16	9.11	9.67	81.30	81.65
China	CHN	116	44.85	2.40	96.27	5.16	56.74	62.51
Congo	COG	2	0.19	0.10	1.08	0.57	66.00	68.28
Czech Republic	CZE	5	0.82	1.67	1.61	3.29	73.57	74.21
Germany	DEU	22	6.63	2.82	12.41	5.29	77.22	77.54
Egypt	EGY	6	1.46	1.68	1.97	2.27	42.73	42.86
France	FRA	25	8.14	2.18	6.45	1.72	79.92	81.24
United Kingdom	GBR	4	0.69	1.69	1.24	3.01	82.89	84.15
Greece	GRC	1	0.25	0.86	0.53	1.84	78.39	80.04
Croatia	HRV	1	0.26	3.44	0.47	6.32	56.40	57.88
Hungary	HUN	7	0.21	0.31	1.05	1.55	70.78	72.25
India	IND	24	5.29	1.41	12.21	3.26	53.99	57.29
Ireland	IRL	2	0.19	0.66	0.28	0.94	62.74	63.91

(continued on next page)

Table A1 (*continued*)

Country name	Abbreviation	Number of cities	Total UVL area in 2016	Total UVL ratio in 2016	Total UVL area in 2021	Total UVL ratio in 2021	Urbanization rate in 2016	Urbanization rate in 2021
Iran	IRN	2	0.13	1.06	0.68	5.80	73.88	76.35
Italy	ITA	10	3.00	2.89	4.11	3.95	69.86	71.35
Japan	JPN	5	0.49	0.42	1.47	1.25	91.46	91.87
Kazakhstan	KAZ	1	0.39	4.38	0.46	5.20	57.26	57.82
Kyrgyzstan	KGZ	1	0.01	0.05	3.49	31.19	35.94	37.15
Korea, Republic Of	KOR	5	0.60	0.34	2.99	1.68	81.56	81.41
Liberia	LBR	1	0.01	0.11	0.12	1.56	50.25	52.57
Lithuania	LTU	3	0.45	0.84	2.07	3.84	67.37	68.25
Morocco	MAR	1	0.01	0.09	2.03	26.57	61.36	64.07
Moldova	MDA	3	0.32	0.64	1.04	2.10	42.51	43.00
Mexico	MEX	1	0.11	1.79	0.10	1.68	79.58	81.02
Netherlands	NLD	2	0.14	1.24	0.48	4.13	90.64	92.57
New Zealand	NZL	1	0.03	0.62	0.04	0.68	86.40	86.79
Poland	POL	8	10.61	1.68	17.13	2.72	60.18	60.08
Portugal	PRT	3	0.14	0.41	0.76	2.19	64.09	66.85
Romania	ROM	13	3.64	2.06	9.52	5.40	53.90	54.33
Russia	RUS	68	59.30	4.11	58.32	4.04	74.16	74.93
Serbia	SEB	4	0.89	2.50	1.00	2.81	55.81	56.65
El Salvador	SLV	1	0.05	0.51	0.05	0.52	70.50	74.12
Suriname	SUR	1	0.02	0.05	0.04	0.08	66.04	66.22
Slovakia	SVK	3	0.68	0.65	1.00	0.96	53.81	53.82
Turkey	TUR	5	8.41	4.82	1.55	0.89	74.13	76.57
Ukraine	UKR	35	20.28	2.38	27.52	3.23	69.15	69.76
Uruguay	URY	1	0.08	1.20	0.08	1.20	95.14	95.60
United States of America	USA	87	28.85	1.39	39.20	1.89	81.86	82.87
South Africa	ZAF	3	0.43	0.81	0.85	1.57	65.34	67.85

Note: Countries are sorted based on the alphabet order of their abbreviations. The unit of total UVL area is km^2. The unit of total UVL ratio is %. The unit of urbanization rate is %.

Appendix B

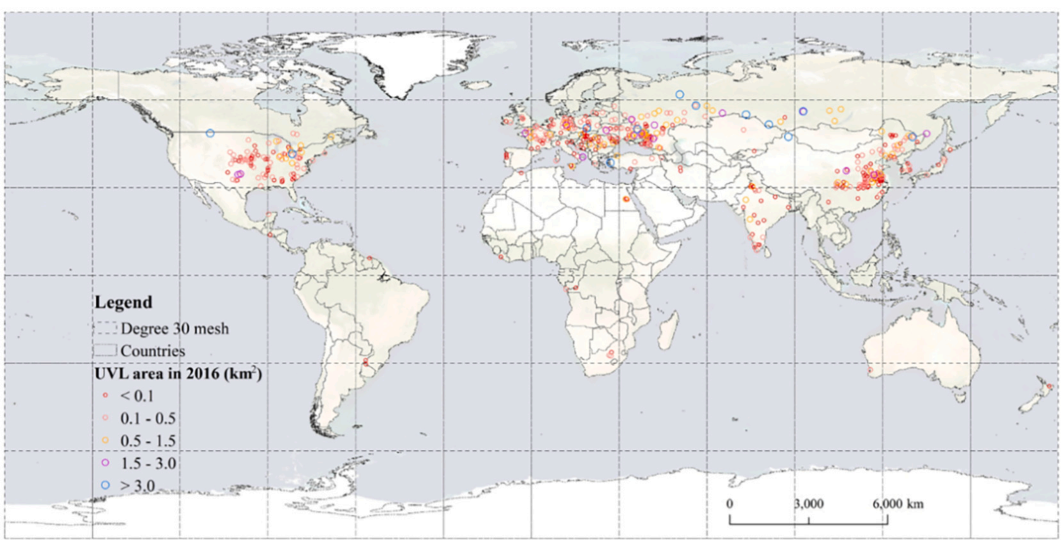

Fig. B1. The total UVL area in 2016 at the city level

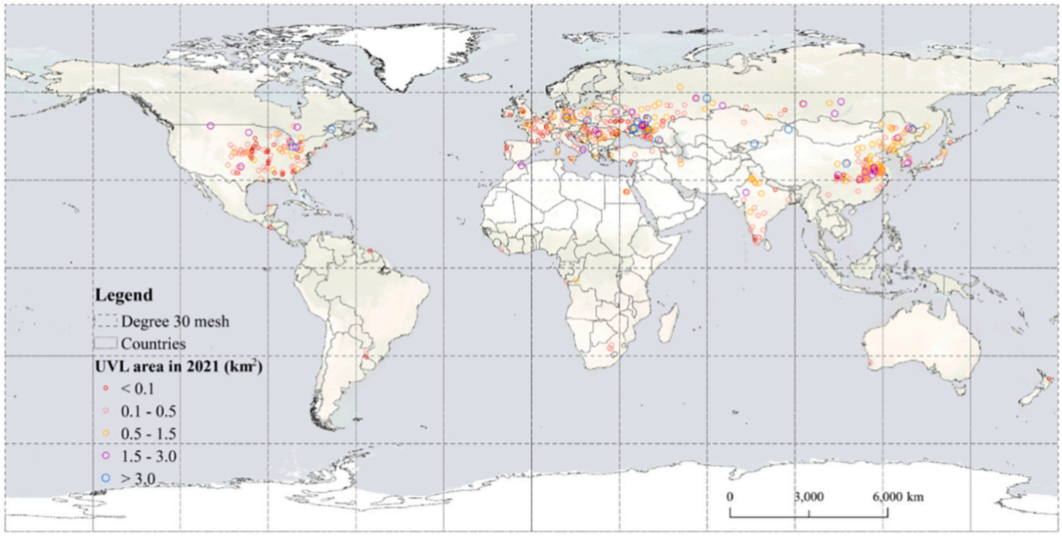

Fig. B2. The total UVL area in 2021 at the city level.

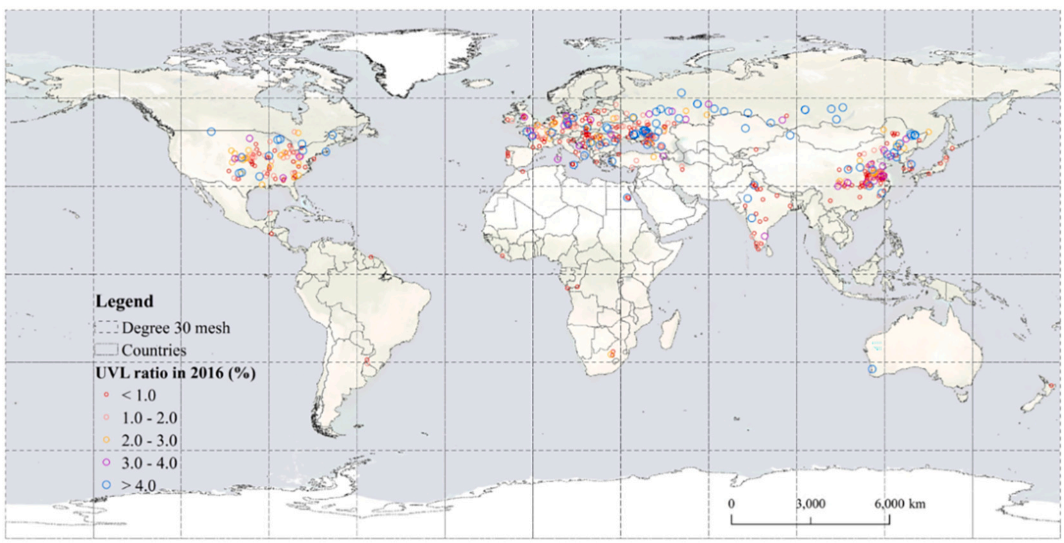

Fig. B3. The UVL ratio in 2016 at the city level.

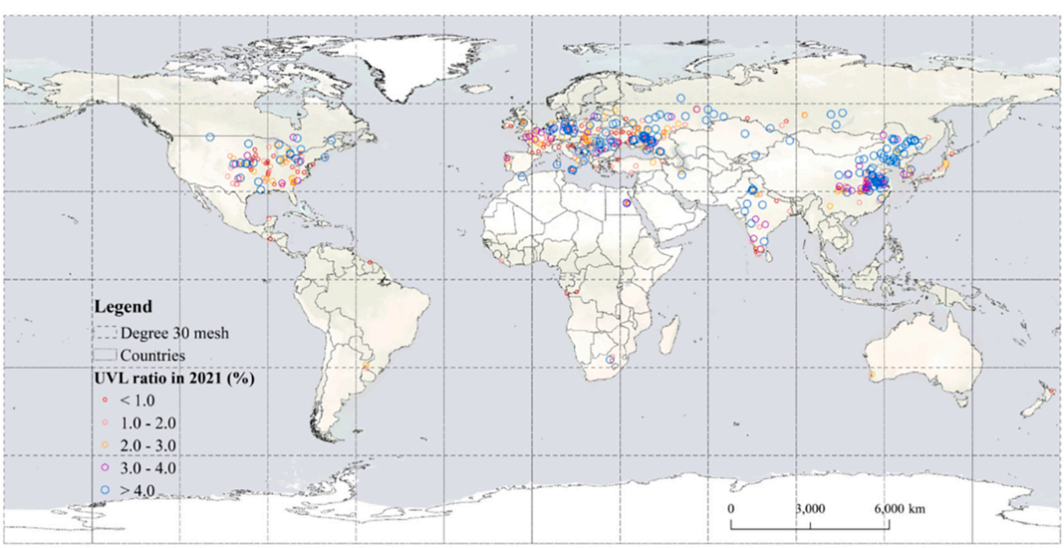

Fig. B4. The UVL ratio in 2021 at the city level.

Appendix C

Table C1
Comparison of deep learning models for auto-identifying UVL between studies.

Research	Number of countries	Number of cities	Trained model	Performance metrics	
				F_2-score	IOU
This study	45	497	Desert	0.892	0.757
			Savanna	0.846	0.591
			Forest	0.846	0.608
			Summer-dry	0.877	0.654
			Winter-dry	0.837	0.563
Mao et al., 2022	1	36	Beijing	0.888	0.719
			Shenzhen	0.852	0.649
			Lanzhou	0.817	0.550
			Hybrid	0.841	0.613

References

Anderson, E.C., Minor, E.S., 2017. Vacant lots: an underexplored resource for ecological and social benefits in cities. Urban For. Urban Green. 21, 146–152. https://doi.org/10.1016/j.ufug.2016.11.015.

Anderson, E.C., Minor, E.S., 2019. Assessing social and biophysical drivers of spontaneous plant diversity and structure in urban vacant lots. Sci. Total Environ. 653, 1272–1281. https://doi.org/10.1016/j.scitotenv.2018.11.006.

Batty, M., 2022. The shape of future cities: three speculations. Trans. Urban Data Sci. Technol. 1 (1–2), 7–12. https://doi.org/10.1177/27541231221113945.

Beck, H.E., Zimmermann, N.E., McVicar, T.R., Vergopolan, N., Berg, A., Wood, E.F., 2018. Present and future Köppen-Geiger climate classification maps at 1-km resolution. Sci. Data 5 (1), 1–12. https://doi.org/10.1038/sdata.2018.214.

Blanco, H., Alberti, M., Olshansky, R., Chang, S., Wheeler, S.M., Randolph, J., Watson, V., 2009. Shaken, shrinking, hot, impoverished and informal: emerging research agendas in planning. Prog. Plan. 72 (4), 195–250. https://doi.org/10.1016/j.progress.2009.09.001.

Chen, G., Li, C., Wei, W., Jing, W., Woźniak, M., Blažauskas, T., Damaševičius, R., 2019. Fully convolutional neural network with augmented atrous spatial pyramid pool and fully connected fusion path for high resolution remote sensing image segmentation. Appl. Sci. 9 (9), 1816. https://doi.org/10.3390/app9091816.

Cheng, Z., Wang, J., Zhu, K., Ge, Y., Zhou, C., 2022. Evaluating spatial statistical and machine learning models in urban dynamic population mapping. Trans. Urban Data Sci. Technol. 1 (1–2), 37–55. https://doi.org/10.1177/27541231221114169.

Delken, E., 2008. Happiness in shrinking cities in Germany: A research note. J. Happiness Stud. 9, 213–218.

Duque, J.C., Patino, J.E., Betancourt, A., 2017. Exploring the potential of machine learning for automatic slum identification from VHR imagery. Remote Sens. 9 (9), 895. https://doi.org/10.3390/rs9090895.

Fan, J., Wang, J., Qiu, J., Li, N., 2019. Stage effects of energy consumption and carbon emissions in the process of urbanization: evidence from 30 provinces in China. Energy 276, 127655. https://doi.org/10.1016/j.energy.2023.127655.

Foo, K., Martin, D., Wool, C., Polsky, C., 2013. The production of urban vacant land: relational placemaking in Boston, MA neighborhoods. Cities 35, 156–163. https://doi.org/10.1016/j.cities.2013.06.012.

Frazier, A.E., Bagchi-Sen, S., 2015. Developing open space networks in shrinking cities. Appl. Geogr. 59, 1–9. https://doi.org/10.1016/j.apgeog.2015.02.010.

Gelman, A., Hill, J., Vehtari, A., 2020. Regression and Other Stories, 1st ed. Cambridge University Press.

Hollander, J.B., Pallagst, K., Schwarz, T., Popper, F.J., 2009. Planning shrinking cities. Prog. Plan. 72 (4), 223–232.

Humphris, I., Rauws, W., Horlings, L., 2024. Planning in a place of co-becoming: informal and more-than-human placemaking in Scottish vacant land policy. Cities 150, 105036. https://doi.org/10.1016/j.cities.2024.105036.

Katz, D.S.W., Carey, T.S., 2014. Heterogeneity in ragweed pollen exposure is determined by plant composition at small spatial scales. Sci. Total Environ. 485, 435–440. https://doi.org/10.1016/j.scitotenv.2014.03.099.

Kim, G., Miller, P.A., Nowak, D.J., 2018. Urban vacant land typology: a tool for managing urban vacant land. Sustain. Cities Soc. 36, 144–156. https://doi.org/10.1016/j.scs.2017.09.014.

Kim, G., Newman, G., Jiang, B., 2020. Urban regeneration: community engagement process for vacant land in declining cities. Cities 102, 102730. https://doi.org/10.1016/j.cities.2020.102730.

Kobayashi, T., Ikaruga, S., 2016. Occurrence factors of large vacant lots in central districts and their utilization by local governments in Japan. Front. Arch. Res. 5 (4), 393–402. https://doi.org/10.1016/j.foar.2016.09.006.

Lee, J., Newman, G., Park, Y., 2018. A comparison of vacancy dynamics between growing and shrinking cities using the land transformation model. Sustainability 10 (5), 1513. https://doi.org/10.3390/su10051513.

Li, W., Zhou, W., Bai, Y., Pickett, S.T., Han, L., 2018. The smart growth of Chinese cities: opportunities offered by vacant land. Land Degrad. Dev. 29 (10), 3512–3520. https://doi.org/10.1002/ldr.3125.

Li, W., Wang, D., Li, H., Wang, J., Zhu, Y., Yang, Y., 2019. Quantifying the spatial arrangement of underutilized land in a rapidly urbanized rust belt city: the case of Changchun city. Land Use Policy 83, 113–123. https://doi.org/10.1016/j.landusepol.2019.01.032.

Li, X., Gong, P., Zhou, Y., Wang, J., Bai, Y., Chen, B., Zhu, Z., 2020. Mapping global urban boundaries from the global artificial impervious area (GAIA) data. Environ. Res. Lett. 15, 094044 https://doi.org/10.1088/1748-9326/ab9be3.

Li, Z., Long, Y., 2018. An analysis on variation of quality of street space in shrinking cities based on dynamic street view pictures recognition: a case study of Qiqihar. Urban. Arch. 275 (6), 21–25. In Chinese. doi: 10.19892/j.cnki.csjz.2018.06.004.

Liu, Z., Zhao, H., Li, S., Chen, Y., Yao, E., 2022. Understanding evolution process of community-embedded elderly care facilities with big data: a spatiotemporal analytical framework. Trans. Urban Data Sci. Technol. 1 (3–4), 142–163. https://doi.org/10.1177/27541231221136406.

Lokhande, T., Xie, Y., 2023. Spatial spillover effects of urban decline in Southeast Michigan. Appl. Geogr. 158, 103031 https://doi.org/10.1016/j.apgeog.2023.103031.

Long, Y., Zhai, W., Shen, Y., Ye, X., 2018. Understanding uneven urban expansion with natural cities using open data. Landsc. Urban Plan. 177, 281–293. https://doi.org/10.1016/j.landurbplan.2017.05.008.

Ma, Y., Su, N., Tu, T., 2023. Urban public space quality evaluation methods and practices in China. Trans. Urban Data Sci. Technol. 2 (2–3), 59–80. https://doi.org/10.1177/27541231231166095.

Mao, L., Zheng, Z., Meng, X., Zhou, Y., Zhao, P., Yang, Z., Long, Y., 2022. Large-scale automatic identification of urban vacant land using semantic segmentation of high-resolution remote sensing images. Landsc. Urban Plan. 222, 104384 https://doi.org/10.1016/j.landurbplan.2022.104384.

Martinez-Fernandez, C., Audirac, I., Fol, S., Cunningham-Sabot, E., 2012. Shrinking cities: urban challenges of globalization. Int. J. Urban Reg. Res. 36 (2), 213–225. https://doi.org/10.1111/j.1468-2427.2011.01092.x.

Meng, X., Jiang, Z., Wang, X., Long, Y., 2021a. Shrinking cities on the globe: evidence from Landscan 2000–2019. Environ. Plann. A Econ. Space 53 (6), 1244–1248. https://doi.org/10.1177/0308518X211006118.

Meng, X., Ma, S., Meng, X., Xiang, W., Kan, C., Wu, K., Long, Y., 2021b. Classification of shrinking cities in China using Baidu big data. Acta Geograph. Sin. 76 (10), 2477–2488. In Chinese. doi: 10.11821/dlxb202110010.

Míguez, F., Gómez-Sagasti, M.T., Hernández, A., Artetxe, U., Blanco, F., Castañeda, J.H., Becerril, J.M., 2020. In situ phytomanagement with Brassica napus and bio-stabilised municipal solid wastes is a suitable strategy for redevelopment of vacant urban land. Urban For. Urban Green. 47, 126550 https://doi.org/10.1016/j.ufug.2019.126550.

Németh, J., Langhorst, J., 2014. Rethinking urban transformation: temporary uses for vacant land. Cities 40, 143–150. https://doi.org/10.1016/j.cities.2013.04.007.

Newman, G.D., Bowman, A.O.M., Jung Lee, R., Kim, B., 2016. A current inventory of vacant urban land in America. J. Urban Des. 21 (3), 302–319. https://doi.org/10.1080/13574809.2016.1167589.

Oswalt, P., Rieniets, T., 2006. Atlas of shrinking cities. Hatje Cantz.

Pagano, M.A., Bowman, A.O.M., 2000. Vacant Land in Cities: An Urban Resource. Brookings Institution, Center on Urban and Metropolitan Policy, Washington, DC.

Pallagst, K., 2009. The future of shrinking cities: problems, patterns and strategies of urban transformation in a global context. In: Institute of Urban and Regional Development, Center for Global Metropolitan Studies, and the Shrinking Cities International Research Network Monograph Series. Retrieved from: https://api.semanticscholar.org/CorpusID:129801674.

Park, Y., Newman, G.D., Lee, J.E., Lee, S., 2021. Identifying and comparing vacant housing determinants across South Korean cities. Appl. Geogr. 136, 102566 https://doi.org/10.1016/j.apgeog.2021.102566.

Pearsall, H., 2017. Staying cool in the compact city: vacant land and urban heating in Philadelphia, Pennsylvania. Appl. Geogr. 79, 84–92. https://doi.org/10.1016/j.apgeog.2016.12.010.

Salvati, L., Zambon, I., Chelli, F.M., Serra, P., 2018. Do spatial patterns of urbanization and land consumption reflect different socioeconomic contexts in Europe? Sci. Total Environ. 625, 722–730. https://doi.org/10.1016/j.scitotenv.2017.12.341.

Sarkar, A., Jana, A., 2023. Interpreting the energy choices and environmental satisfaction determinants in low-income housing typologies: cases from slums and slum rehabilitation housing of Mumbai. India. Cities 143, 104576. https://doi.org/10.1016/j.cities.2023.104576.

Schetke, S., Haase, D., 2008. Multi-criteria assessment of socio-environmental aspects in shrinking cities: experiences from eastern Germany. Environ. Impact Assess. Rev. 28 (7), 483–503. https://doi.org/10.1016/j.eiar.2007.09.004.

Shukla, A., Jain, K., 2020. Automatic extraction of urban land information from unmanned aerial vehicle (UAV) data. Earth Sci. Inf. 13 (4), 1225–1236. https://doi.org/10.1007/s12145-020-00498-x.

Smith, J.P., Li, X., Turner II, B.L., 2017. Lots for greening: identification of metropolitan vacant land and its potential use for cooling and agriculture in Phoenix, AZ, USA. Appl. Geogr. 85, 139–151. https://doi.org/10.1016/j.apgeog.2017.06.005.

Song, X., Li, X., 2019. Urban vacant land: connotation and research direction. China Land Sci. 33 (6), 71–79. In Chinese. doi: 10.11994/zgtdkx.20190529.162126.

Song, X., Wen, M., Shen, Y., Feng, Q., Xiang, J., Zhang, W., Wu, Z., 2020. Urban vacant land in growing urbanization: an international review. J. Geogr. Sci. 30 (4), 669–687. https://doi.org/10.1007/s11442-020-1749-0.

Sperandelli, D.I., Dupas, F.A., Dias Pons, N.A., 2013. Dynamics of urban sprawl, vacant land, and green spaces on the metropolitan fringe of São Paulo, Brazil. J. Urban Plann. Dev. 139 (4), 274–279. https://doi.org/10.1061/(ASCE)UP.1943-5444.0000154.

UNIDO (United Nations Industrial Development Organization), 2022. Factsheet: Asia and Oceania highlights from the international yearbook of industrial statistics 2023. Retrieved from: https://www.unido.org/sites/default/files/unido-publications/2023-12/documents_Yearbook_2023_UNIDO_IndustrialStatistics_Yearbook_2023_AsiaO.pdf.

Wang, X., Long, Y., 2023. Future shrinking cities on the globe: a projection map for 2020–2100 based on global gridded population dataset. Environ. Plann. B Urban Anal. City Sci. 50 (7), 1994–1997. https://doi.org/10.1177/23998083231186153.

Wang, X., Meng, X., Long, Y., 2022a. Projecting 1 km-grid population distributions from 2020 to 2100 globally under shared socioeconomic pathways. Sci. Data 9 (1), 563. https://doi.org/10.1038/s41597-022-01675-x.

Wang, X., Li, Y., Li, W., Li, H., Long, Y., 2024. Quality assessment of urban public space from the perspective of urban renewal: exploration based on mobile sensing. Urban Plann. Int. 39 (01), 21–29. In Chinese. doi: 10.19830/j.upi.2023.558.

Wang, Z., Wang, J., Yang, K., Wang, L., Su, F., Chen, X., 2022b. Semantic segmentation of high-resolution remote sensing images based on a class feature attention mechanism fused with Deeplabv3+. Comput. Geosci. 158, 104969 https://doi.org/10.1016/j.cageo.2021.104969.

Wiechmann, T., 2008. Errors expected—aligning urban strategy with demographic uncertainty in shrinking cities. Int. Plan. Stud. 13 (4), 431–446.

Xiong, C., Zhang, Y., Liu, X., Luan, Q., Wei, S., 2021. Urban vacant land in rapidly urbanized areas: status, micro-level drivers, and implications. J. Chin. Gov. 6 (4), 554–577. https://doi.org/10.1080/23812346.2021.1971420.

Xu, S., Ehlers, M., 2022. Automatic detection of urban vacant land: an open-source approach for sustainable cities. Comput. Environ. Urban. Syst. 91, 101729 https://doi.org/10.1016/j.compenvurbsys.2021.101729.

Yu, H., Lee, J., 2023. Analysis of factors affecting the occurrence of vacant houses according to vacant house classification: Shizuoka Prefecture. Japan. Appl. Geogr. 151, 102872 https://doi.org/10.1016/j.apgeog.2023.102872.

Yuan, X., Shi, J., Gu, L., 2021. A review of deep learning methods for semantic segmentation of remote sensing imagery. Expert Syst. Appl. 169, 114417 https://doi.org/10.1016/j.eswa.2020.114417.

Zhai, W., Jiang, Z., Meng, X., Zhang, X., Zhao, M., Long, Y., 2022. Satellite monitoring of shrink- ing cities on the globe and containment solutions. iScience 25 (6), 104411. https://doi.org/10.1016/j.isci.2022.104411.

Zhang, W., Li, Y., Zheng, C., 2023. The distribution characteristics and driving mechanism of vacant land in Chengdu, China: a perspective of urban shrinkage and expansion. Land Use Policy 132, 106812. https://doi.org/10.1016/j.landusepol.2023.106812.

Zhao, S., Liu, S., Xu, C., Yuan, W., Sun, Y., Yan, W., Fang, J., 2018. Contemporary evolution and scaling of 32 major cities in China. Ecol. Appl. 28 (6), 1655–1668. https://doi.org/10.1002/eap.1760.